Recent decoupling of global mean sea level rise from decadal scale climate variability

Reik V. Donner[1,2,3] **and Susana Barbosa**[1]

[1]INESC TEC, Campus da FEUP, Rua Dr Roberto Frias, 4200-465 Porto, Portugal
[2]Department of Water, Environment, Construction and Safety, Magdeburg–Stendal University of Applied Sciences, Breitscheidstraße 2, 39114 Magdeburg, Germany
[3]Research Department IV – Complexity Science, Potsdam Institute for Climate Impact Research (PIK) – Member of the Leibniz Association, Telegrafenberg A31, 14473 Potsdam, Germany

Key Points:

- Long-term changes in altimetry derived global mean sea level well explained by Pacific Decadal Variability until mid-2019
- Recent decoupling of global mean sea level from low-frequency climate variability mode
- Unprecedented increase in global mean sea level rise in recent years

Corresponding author: Susana A. M. Barbosa, `susana.a.barbosa@inesctec.pt`

Abstract

Sea level rise is among the most challenging consequences of global climate change. To better understand recent changes in global mean sea level trends, we analyze global satellite altimetry data from December 1992 until late 2024. When correcting for an average linear trend and decomposing the residual into contributions at different time scales, we find a striking co-variability between low-frequency modulations of global mean sea level rise and the Pacific Decadal Oscillation (PDO), which persists from the beginning of the record until about 2019. By contrast, this association has been lost during the last years, where a PDO based extrapolation would have anticipated a slowing down of sea level rise while observations revealed an upward trend in the rate of change. This indicates that multidecadal coupled atmosphere-ocean processes in the Pacific have been recently replaced by other factors as drivers of low-frequency modulations of global mean sea level rise.

Plain Language Summary

We analyze global satellite data of sea level rise during the last about 32 years. By subtracting a simple statistical model with a constant rate of change, we are able to study temporal changes in global sea level trends, which can result from different possible factors. Our results demonstrate that for most of the past three decades, decadal scale modulations in global mean sea level trends have been tightly coupled to a dominant climate variability mode in the Pacific ocean. By contrast, this strong link has got lost during the last years, where climate forcing would have anticipated a slowing down of global sea level rise while observations rather indicate an increasing rate of change. In this regard, from the perspective of Pacific decadal climate variability as a strong driver of global mean sea level rise modulations during the past decades, the recent acceleration of sea level rise has been unprecedented.

1 Introduction

Global mean sea level (GMSL) reflects in an integrated way the overall variability in the Earth's climate system, and is currently rising at an average rate of 3.3 mm/yr, as estimated from the fit of a linear model to the satellite altimetry record (Guérou et al., 2023).

Understanding GMSL variations beyond the overall trend is critical to interpret long-term patterns. At interannual to decadal timescales variability in GMSL is mainly driven by steric changes in ocean heat content and barystatic variations of water mass (Gregory et al., 2019), with the El Niño-Southern Oscillation (ENSO) climate mode contributing about equally to both (B. D. Hamlington et al., 2020). Quantifying the contribution to GMSL of internal multidecadal climate variability assists in the assessment of anthropogenic contributions and its role in current GMSL acceleration (Chen et al., 2017; Nerem et al., 2018; B. Hamlington et al., 2024).

In this work we focus on the co-variability between GMSL and the Pacific Decadal Variability as expressed by the Pacific Decadal Oscillation (PDO) index (Mantua et al., 1997; Y. Zhang et al., 1997). The PDO affects sea level through changes in wind stress, sea surface temperature (SST), and ocean circulation patterns. Local and regional impacts of PDO on sea level variability have been reported in various studies based on tide gauge data (Deepa & Gnanaseelan, 2021) as well as satellite altimetry (Cheng et al., 2015; Deepa et al., 2018; Y. Zhang et al., 2018). For the Pacific Ocean, several studies have shown a close association between the PDO and regional sea level (Cummins et al., 2005; Merrifield et al., 2012; X. Zhang & Church, 2012; Moon et al., 2015; Han et al., 2014; B. D. Hamlington et al., 2014; Meng et al., 2019). For GMSL, (B. Hamlington et al., 2013) used a sea level reconstruction to study trends in sea level since 1950, concluding that the PDO causes acceleration and deceleration in GMSL on decadal time scales.

By quantifying the co-variability of PDO index and GMSL over the satellite altimetry record, we demonstrate that the low-frequency variability superposed to (linear) GMSL rise is largely consistent with PDO, but exhibiting a complete decoupling after 2019. Thus GMSL rise estimated by accounting for low-frequency climate variability is unprecedented since 2019, supporting a significant acceleration in the rise of global mean sea level.

2 Materials and Methods

2.1 Data

We use the global mean sea level time series with seasonal signals removed that is provided by NOAA Laboratory for Satellite Altimetry based on TOPEX/Poseidon (T/P), Jason-1, Jason-2, Jason-3, and Sentinel-6MF satellite missions. All standard geophysical corrections have been applied to the altimetry measurements, including the inverted barometer correction. Only satellite measurements between 66°S and 66°N are included. The time series has an original temporal resolution of 10-days, but is aggregated to monthly values by computing the median, in order to facilitate the joint analysis with monthly-based climate indices.

For the PDO data we use the monthly PDO index provided bcy NOAA's National Centers for Environmental Information which is based on NOAA's extended reconstruction of SSTs (ERSST Version 5) for the same period as the satellite altimetry time series (December 1992 to September 2024).

2.2 Statistical methods

Linear trends are estimated in this work using the conventional ordinary least squares framework, but taking autocorrelation in the time series into account by considering a first order autoregressive correlation structure, which is equivalent to computing an effective sample size from the autocorrelation coefficient at the first lag, as for example in (Maul & Martin, 1993). This approach does not change the slope estimate but ensures more realistic (larger) confidence bands by accounting for time series autocorrelation.

Filtering is performed by a level $J = 3$ multiresolution analysis in the wavelet domain based on the maximal overlap discrete wavelet transform (D. Percival & Mojfeld, 1997; D. B. Percival, 2008) using a Daubechies Least Asymmetric filter (Daubechies, 1988) with reflection boundary conditions. This is an additive decomposition - no information is lost, as the sum of all components corresponds to the original time series - producing J detail components D_j reflecting variability on scales between $2^{(j-1)}$ and 2^j months ($j = 1, ..., J$), and a long-term component S_J reflecting variability on scales $> 2^J$.

3 Results

The monthly time series of global mean sea level is presented in Figure 1 (top), together with the corresponding linear trend of 3.10 ± 0.087 mm/year (the uncertainty range would be only ± 0.023 mm/year if autocorrelation were not taken into account). Subtracting this linear trend from the global mean sea level time series yields the detrended time series shown in Figure 1 (middle), which exhibits a clearly nonrandom pattern of multi-year variability, characterized by a tendency toward decreasing values until approximately 2010, followed by increasing values thereafter, superimposed on high-frequency variability.

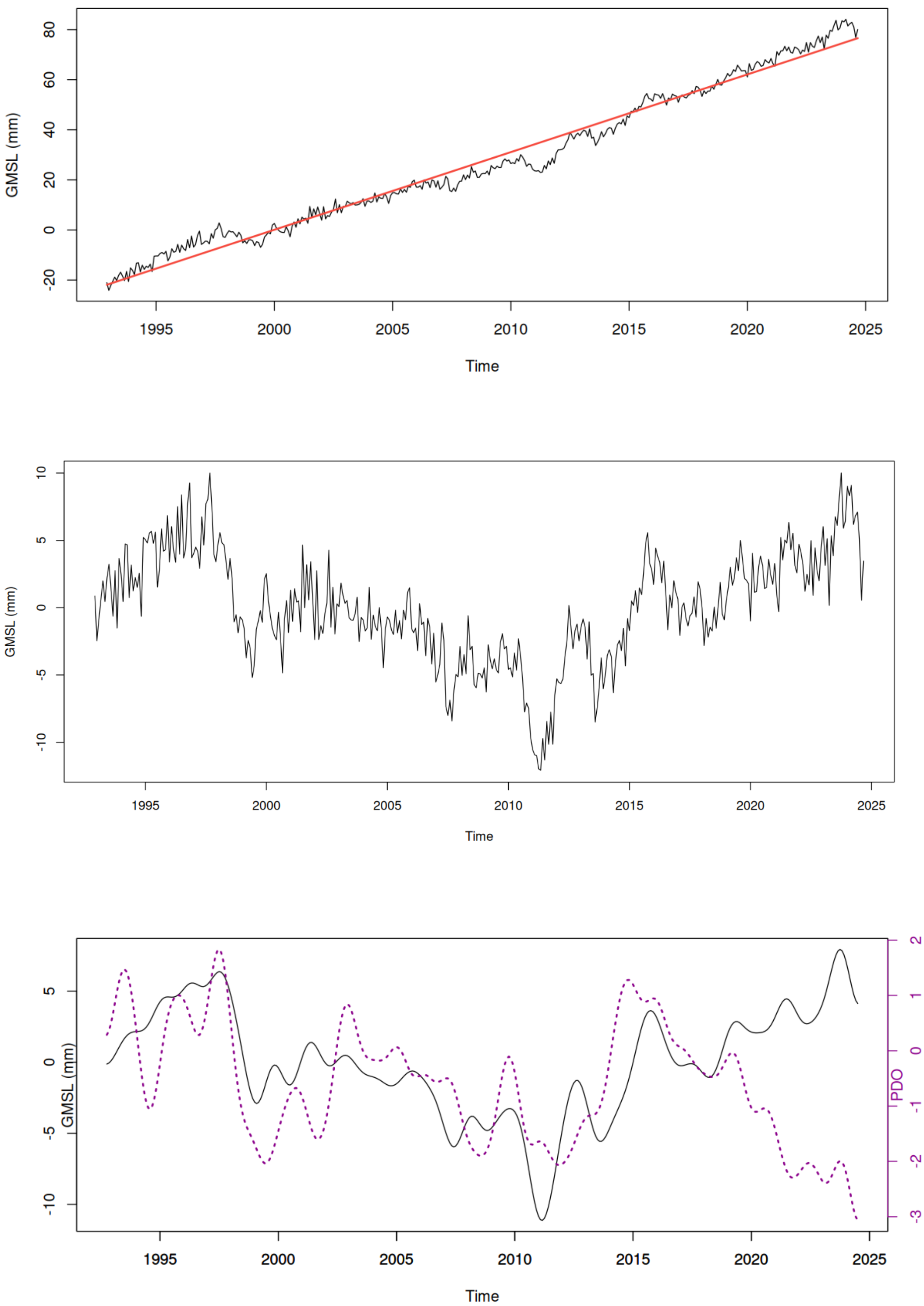

Figure 1. Top: Monthly global mean sea level (black) from satellite altimetry together with a linear trend (red) obtained from standard ordinary least squares regression for the time period 1992-2024. Middle: Residual monthly global mean sea level after linear detrending. Bottom: Wavelet-filtered low-frequency variability component of the linearly detrended global mean sea level (black) and the PDO index (purple).

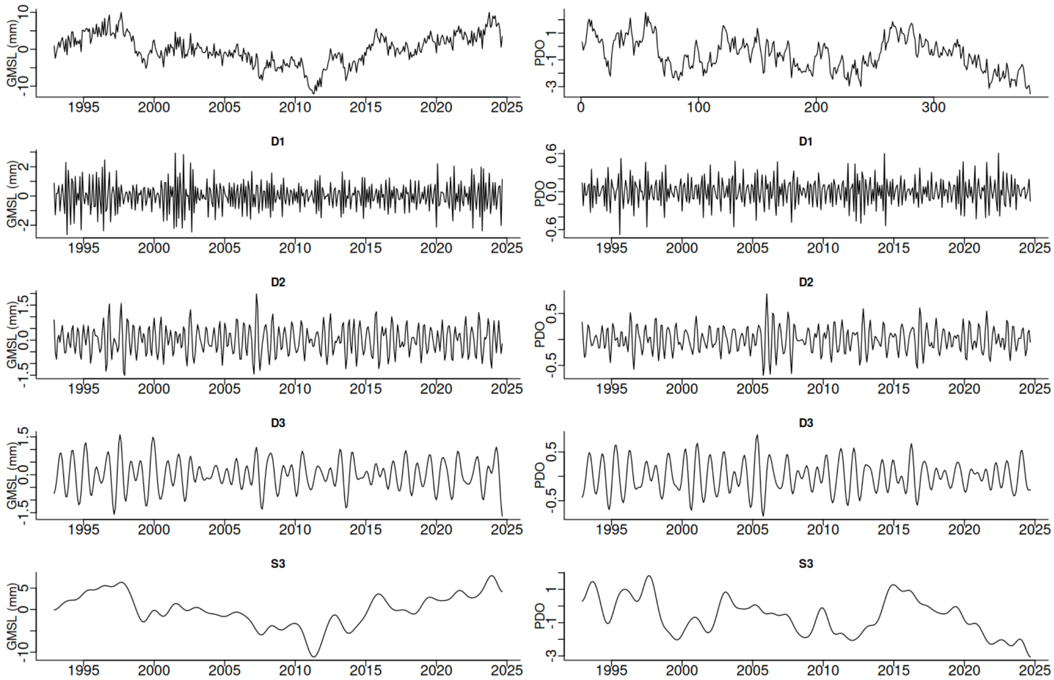

Figure 2. Discrete wavelet decomposition of the linearly detrended GMSL (left panels) and the PDO index (right panels). From top to bottom, the individual panels show the original time series, the detail coefficients of the first three decomposition levels (D1, D2 and D3, corresponding to time scales of one to two, two to four, and four to eight months, respectively), and the low-frequency residual S3 capturing inter-annual to multi-decadal variability components.

3.1 Low-frequency variability

In order to focus the analysis on low-frequency variability, the time series of the detrended global mean sea level is filtered using a wavelet-based decomposition (Figure 2, left panels) that yields the low-frequency component displayed in Figure 1 (bottom, solid black line). The low-frequency variability of the PDO time series is extracted in the same way (Figure 2, right panels) and is represented in Figure 1 (bottom, dotted purple line). The joint plot of the low frequency variability of the monthly GMSL and PDO in Figure 1 shows a very similar pattern up to about 2019 but diverges afterwards, with an upward trend in the low-frequency variability of the GMSL (i.e., an acceleration of GMSL) and a decrease in the low-frequency variability component of the PDO index from about 2019 onward.

The co-variability of GMSL and PDO low-frequency patterns is quantified by computing the correlation coefficient between the two time series. Considering the complete period, from December 1992 to September 2024, the correlation coefficient is small (0.23). However, as shown in Figure 1 (bottom panel) the co-variability seems to differ substantially in the last portion of the time series. This is confirmed by computing the correlation coefficient starting at the same time (December 1992) but for different end points, varying from June 2016 to the complete time series (September 2024). The correlation between the two patterns was about 0.65 up to September 2019, substantially decreasing afterwards (Figure 3).

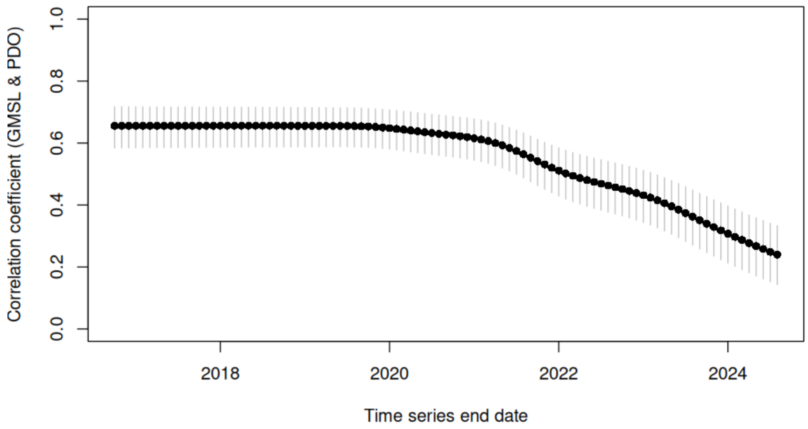

Figure 3. Correlation coefficient between GMSL and PDO low-frequency components as a function of the end point taken for the time series. The points denote the estimated correlation coefficient and the vertical bars the corresponding 95% confidence interval (ignoring variance inflation due to serial dependency in the time series).

3.2 Linear statistical model for GMSL trend modulations

The correlation between low-frequency patterns of GMSL and PDO suggests the possibility of developing a linear model between the two time series, enabling to predict GMSL low-frequency behavior (i.e., inter-annual to multi-decadal modulations of the average rate of GMSL rise) based on the PDO index. From Figure 3 the maximum correlation coefficient is obtained when taking the two time series from December 1992 to July 2018, thus this period would be a natural choice for the modeling period. However, because the correlation values decrease slowly up to about 2021, and to ascertain how modeling results would be affected by the specific choice of end point, the linear model for predicting GMSL from the PDO is estimated considering different end points, from July 2018 to February 2021. For example, taking as end-point July 2018, the linear model describing GMSL low-frequency modulations as a function of the PDO is estimated from the low-frequency patterns of GMSL and PDO up to July 2018, and out-of-smample predictions are produced from that model for August 2018 to September 2024 (without using any data from that period). The procedure is then repeated by estimating a linear model up to August 2018 and then predicting GMSL from the model from September 2018 to September 2024, etc.

The results are summarized in Figure 4 showing the low-frequency pattern of GMSL from the satellite altimetry data (black line) and the GMSL line that would be obtained from the linear model relating GMSL and the PDO (blue line), with the corresponding uncertainty band. From July 2018 onward, the model is used for predicting GMSL based exclusively on PDO data, with the corresponding prediction interval represented by the gray band. The spread in the blue prediction line reflects the fact that several predictions are made, for each of the end points considered, but it is significantly narrower than the 95% prediction interval in gray representing the uncertainty in the linear model prediction, indicating that the results are robust to the choice of the end point used in the model.

3.3 GMSL trends

The linear model presented in the previous section yields a statistically modelled time series describing the low-frequency variability in GMSL based exclusively on the

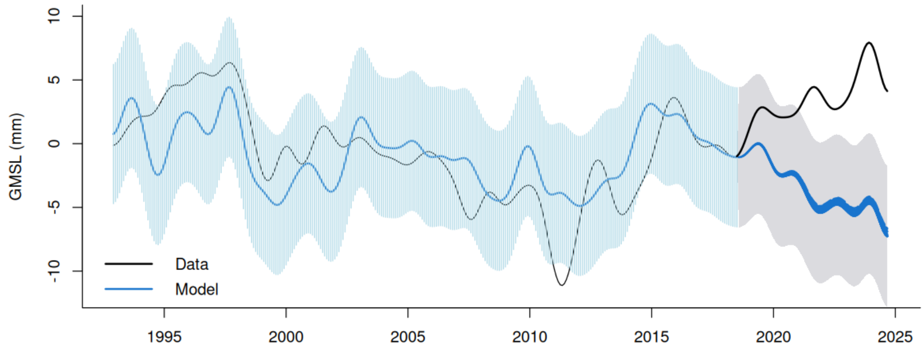

Figure 4. Low-frequency variability component of GMSL from the satellite altimetry data (black) and estimated from a linear model relating GMSL and the PDO (blue), with corresponding uncertainty band. The grey shaded area denotes de 95% prediction interval for prediction of GMSL from August 2018 to September 2024 based exclusively on the PDO.

PDO index. The full variability (rather than just the low-frequency one) is recovered by adding back to this time series the high frequency components from the wavelet decomposition (D_1+D_2+D_3). Furthermore, detrending is reverted by adding back the same the linear trend that was originally removed (Figure 1, top). The resulting time series, along with the original GMSL time series, is shown in Figure 5. The two time series are very similar except for the most recent period, in which the observed GMSL increases at a comparatively higher rate that is incompatible with what would be expected from the historical association between GMSL and the PDO. More specifically, the linear trend obtained from the modelled time series, of 2.98±0.034 mm/year, is significantly lower than the actual trend from the GMSL altimetry time series. Furthermore, the fit of a quadratic model to the GMSL time series yields an acceleration of 0.08 mm/year^2 while for the modelled time series the acceleration is not statistically significant.

4 Discussion and Conclusions

Our anaysis has demonstrated that for most of the last more than three decades, the low-frequency variability in GMSL has closely followed the variability of the PDO climate mode. Up to mid 2019, a simple linear model relating the two signals is able to successfully describe the low-frequency variability in GMSL based only on the PDO signal. The only short period with a slight, yet statistically significant mismatch has been related to the 2010–2011 La Niña event (Figure 4), which has lead to a temporary reversal of the direction of GMSL trends. This reversal is not captured by the PDO based model, which rather focuses on variability on even longer time scales.

While the simple PDO based linear statistical model describes low-frequency modulations of GMSL rise reasonably well for most of the available altimetry record, after mid 2019, the correlation between the two signals starts to decrease, first slowly and then in a more obvious way (Figure 3). In modelling the co-variability between GMSL and PDO a range of time points (from July 2018 to February 2021) was considered as candidates for the decoupling of the two signals, in order to assess the dependence of the results on the assumed specific decoupling time. The model results are very robust, and are not markedly affected by the assumed time for the break in the correlation between

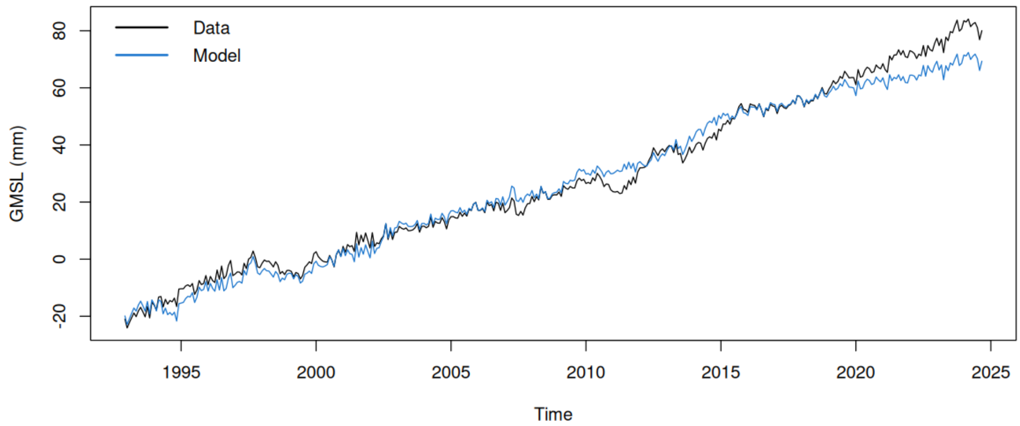

Figure 5. GMSL from the satellite altimetry data (black) and from the linear model relating GMSL and the PDO (blue).

the two signals, since irrespective of the specific time considered the GMSL modulations predicted from the historical relation with the PDO have a very similar pattern within the model's uncertainty (Figure 4, grey band). Thus, assuming that the association between low-frequency variability in GMSL and PDO was still valid after mid-2019, the low-frequency variability in GMSL modulations would have decreased, following the PDO pattern, rather than increased, as evidenced by the satellite altimetry observations.

The satellite altimetry data used in the present study was obtained from the NOAA Laboratory for Satellite Altimetry, ensuring consistency in the processing of the satellite data. Thus, the identified decoupling between GMSL and the low-frequency climate variability represented by the PDO is unlikely to be related to an instrumental effect or some issue with the altimetry observations used to produce the GMSL time series. The specific cause of the distinct behaviour of GMSL relative to the PDO requires further investigation, but the robust identification of the decoupling between the two signals already allows to conclude that the acceleration in GMSL observed in recent years (B. Hamlington et al., 2024) is unprecedented and not explainable by low-frequency climate variability. Follow-up studies may look deeper into the spatial fingerprint of this decoupling, providing a possible way to identifying the underlying mechanisms.

Open Research Section

All data and software code used in the paper are available in the Zenodo repository (https://doi.org/10.5281/zenodo.15270372).

Acknowledgments

This work has been financially supported by INESC TEC via the International Visiting Researcher Programme 2024, and by the Portuguese funding agency, FCT - Fundação para a Ciência e a Tecnologia, within project UIDB/50014/2020. DOI 10.54499/UIDB/50014/2020 https://doi.org/10.54499/uidb/50014/2020. It is also co-financed by Component 5 - Capitalization and Business Innovation, integrated in the Resilience Dimension of the Recovery and Resilience Plan within the scope of the Recovery and Resilience Mechanism (MRR) of the European Union (EU), framed in the Next Generation EU, for the period

2021 - 2026, within project NewSpacePortugal, with reference 11. RVD additionally acknowledges funding by the German Federal Ministry of Education and Research within the JPI Oceans / JPI Climate NextG-Climate Science project "ROADMAP – The role of ocean dynamics and ocean-atmosphere interactions in driving climate variations and future projections of impact-relevant extreme events" (grant no. 01LP2002B). Altimetry data are provided by NOAA Laboratory for Satellite Altimetry.

References

Chen, X., Zhang, X., Church, J. A., Watson, C. S., King, M. A., Monselesan, D., ... Harig, C. (2017). The increasing rate of global mean sea-level rise during 1993–2014. *Nature Climate Change*, *7*(7), 492-495.

Cheng, Y., Plag, H., Hamlington, B., Xu, Q., & He, Y. (2015). Regional sea level variability in the bohai sea, yellow sea, and east china sea. *Continental Shelf Research*, *111*, 95-107. doi: 10.1016/J.CSR.2015.11.005

Cummins, P. F., Lagerloef, G. S. E., & Mitchum, G. (2005). A regional index of northeast pacific variability based on satellite altimeter data. *Geophysical Research Letters*, *32*(17). doi: https://doi.org/10.1029/2005GL023642

Daubechies, I. (1988). Orthonormal Bases of Compactly Supported Wavelets. *Communications on Pure and Applied Mathematics*, *41*, 909–996.

Deepa, J. S., Deepa, J. S., Gnanaseelan, C., Mohapatra, S., Mohapatra, S., Chowdary, J., ... Parekh, A. (2018). The tropical indian ocean decadal sea level response to the pacific decadal oscillation forcing. *Climate Dynamics*, *52*, 5045-5058. doi: 10.1007/s00382-018-4431-9

Deepa, J. S., & Gnanaseelan, C. (2021). The decadal sea level variability observed in the indian ocean tide gauge records and its association with global climate modes. *Global and Planetary Change*, *198*, 103427. doi: 10.1016/J.GLOPLACHA.2021.103427

Gregory, J. M., Griffies, S. M., Hughes, C. W., Lowe, J. A., Church, J. A., Fukimori, I., ... others (2019). Concepts and terminology for sea level: Mean, variability and change, both local and global. *Surveys in Geophysics*, *40*, 1251–1289.

Guérou, A., Meyssignac, B., Prandi, P., Ablain, M., Ribes, A., & Bignalet-Cazalet, F. (2023). Current observed global mean sea level rise and acceleration estimated from satellite altimetry and the associated measurement uncertainty. *Ocean Science*, *19*(2), 431–451.

Hamlington, B., Bellas-Manley, A., Willis, J., Fournier, S., Vinogradova, N., Nerem, R., ... Kopp, R. (2024). The rate of global sea level rise doubled during the past three decades. *Communications Earth & Environment*, *5*(1), 601.

Hamlington, B., Leben, R., Strassburg, M. W., Nerem, R. S., & Kim, K.-Y. (2013). Contribution of the pacific decadal oscillation to global mean sea level trends. *Geophysical Research Letters*, *40*, 5171 - 5175. doi: 10.1002/grl.50950

Hamlington, B. D., Piecuch, C. G., Reager, J. T., Chandanpurkar, H., Frederikse, T., Nerem, R. S., ... Cheon, S.-H. (2020). Origin of interannual variability in global mean sea level. *Proceedings of the National Academy of Sciences*, *117*(25), 13983–13990.

Hamlington, B. D., Strassburg, M., Leben, R., Han, W., Nerem, R., & Kim, K.-Y. (2014). Uncovering an anthropogenic sea-level rise signal in the pacific ocean. *Nature Climate Change*, *4*(9), 782–785.

Han, W., Meehl, G., Hu, A., Alexander, M., Yamagata, T., Yuan, D., ... Leben, R. (2014). Intensification of decadal and multi-decadal sea level variability in the western tropical pacific during recent decades. *Climate Dynamics*, *43*, 1357-1379. doi: 10.1007/s00382-013-1951-1

Mantua, N. J., Hare, S. R., Zhang, Y., Wallace, J. M., & Francis, R. C. (1997). A Pacific interdecadal climate oscillation with impacts on salmon production*. *Bulletin of the American Meteorological Society*, *78*(6), 1069-1080. doi:

10.1175/1520-0477(1997)078⟨1069:APICOW⟩2.0.CO;2
Maul, G., & Martin, D. (1993). Sea level rise at Key West, Florida, 1846-1992: America's longest intrument record? *Geophysical Research Letters*, *20*(18), 1955–1958.
Meng, L., Zhuang, W., Zhang, W., Ditri, A., & Yan, X. (2019). Decadal sea level variability in the pacific ocean: Origins and climate mode contributions. *Journal of Atmospheric and Oceanic Technology*. doi: 10.1175/JTECH-D-18-0159.1
Merrifield, M. A., Thompson, P. R., & Lander, M. (2012). Multidecadal sea level anomalies and trends in the western tropical pacific. *Geophysical Research Letters*, *39*(13). Retrieved from `https://agupubs.onlinelibrary.wiley.com/doi/abs/10.1029/2012GL052032` doi: 10.1029/2012GL052032
Moon, J., Song, Y., & Lee, H. (2015). Pdo and enso modulations intensified decadal sea level variability in the tropical pacific. *Journal of Geophysical Research*, *120*, 8229-8237. doi: 10.1002/2015JC011139
Nerem, R. S., Beckley, B. D., Fasullo, J. T., Hamlington, B. D., Masters, D., & Mitchum, G. T. (2018). Climate-change–driven accelerated sea-level rise detected in the altimeter era. *Proceedings of the national academy of sciences*, *115*(9), 2022–2025.
Percival, D., & Mojfeld, H. (1997). Analysis of subtidal coastal sea level fluctuations using wavelets. *Journal of the American Statistical Association*, *92*, 868–880.
Percival, D. B. (2008). Analysis of Geophysical Time Series using Discrete Wavelet Transforms: An Overview. In R. V. Donner & S. M. Barbosa (Eds.), (Vol. 112, p. 61–79). Springer Berlin / Heidelberg.
Zhang, X., & Church, J. A. (2012). Sea level trends, interannual and decadal variability in the pacific ocean. *Geophysical Research Letters*, *39*(21). doi: https://doi.org/10.1029/2012GL053240
Zhang, Y., Wallace, J. M., & Battisti, D. S. (1997). ENSO-like interdecadal variability: 1900–93. *Journal of Climate*, *10*(5), 1004 - 1020. doi: 10.1175/1520-0442(1997)010⟨1004:ELIV⟩2.0.CO;2
Zhang, Y., Xie, S., Kosaka, Y., & Yang, J. (2018). Pacific decadal oscillation: Tropical pacific forcing versus internal variability. *Journal of Climate*. doi: 10.1175/JCLI-D-18-0164.1